Higher order acoustoelastic Lamb wave propagation in stressed plates

Ning Pei and Leonard J. Bond

Articles you may be interested in

Derivation of acoustoelastic Lamb wave dispersion curves in anisotropic plates at the initial and natural frames of reference
J. Acoust. Soc. Am. **140**, (2016); 10.1121/1.4964343

Resonant metalenses for flexural waves in plates
J. Acoust. Soc. Am. **140**, (2016); 10.1121/1.4967179

The effect of cubic material nonlinearity on the propagation of torsional wave modes in a pipe
J. Acoust. Soc. Am. **140**, (2016); 10.1121/1.4967828

Modeling and design of two-dimensional membrane-type active acoustic metamaterials with tunable anisotropic density
J. Acoust. Soc. Am. **140**, (2016); 10.1121/1.4966627

Higher order acoustoelastic Lamb wave propagation in stressed plates

Ning Pei and Leonard J. Bond[a)]

Department of Aerospace Engineering and Center for Nondestructive Evaluation, Iowa State University, Ames, Iowa 50011, USA

Modeling and experiments are used to investigate Lamb wave propagation in the direction perpendicular to an applied stress. Sensitivity, in terms of changes in velocity, for both symmetrical and anti-symmetrical modes was determined. Codes were developed based on analytical expressions for waves in loaded plates and they were used to give wave dispersion curves. The experimental system used a pair of compression wave transducers on variable angle wedges, with set separation, and variable frequency tone burst excitation, on an aluminum plate 0.16 cm thick with uniaxial applied loads. The loads, which were up to 600 $\mu\varepsilon$, were measured using strain gages. Model results and experimental data are in good agreement. It was found that the change in Lamb wave velocity, due to the acoustoelastic effect, for the S_1 mode exhibits about ten times more sensitive, in terms of velocity change, than the traditional bulk wave measurements, and those performed using the fundamental Lamb modes. The data presented demonstrate the potential for the use of higher order Lamb modes for online industrial stress measurement in plate, and that the higher sensitivity seen offers potential for improved measurement systems. © *2016 Acoustical Society of America.*
[http://dx.doi.org/10.1121/1.4967756]

I. INTRODUCTION

In a range of metal forming processes, there remains a need for improved online real-time measurements of stress in thin metal plates. Guided waves, which are also known as Lamb waves, have been used to provide one approach to making such measurements nondestructively.[1] The velocity of these waves is sensitive to the effects of texture, anisotropy, temperature, and stress in the plate material. These phenomena all cause changes in the various higher order elastic constants that determine wave velocity and these relationships are known as the acoustoelastic effects.

The feasibility of utilizing the acoustoelastic effect, the relationships between elastic properties and velocities, as a means to investigate texture and stress has long been established.[2,3] An extensive treatment of the fundamental aspects of the topic was provided by Pao *et al.*[4] The phenomena have now been used with ultrasonic waves for measuring both applied and residual stress, and such measurements are established and reported in many studies (e.g., Refs. 5–7). There have been a more limited number of studies that have considered methods to measure residual stress, in process, such as with aluminum plates, and these have included implementations using shear-horizontal (SH) wave Electromagnetic acoustic transducer (EMAT).[8] However, with all these investigations there have been challenges in providing adequate sensitivity, in terms of the accurate time measurement needed for velocity estimation, particularly at lower stress levels where velocity changes are quite small

and where these effects can be of a similar order to those due to temperature and texture.

An alternate, and related approach, to give residual stress characterization has been performed using longitudinal critically refracted (LCR) waves,[9–11] which are also known as creeping waves. The LCR wave is usually generated at the first critical angle of the incident wave at the interface, and it then propagates just below the surface of the specimen. These waves are found to be most sensitive to the stress that is aligned in the direction of wave propagation. When looking at the case of thin plates it is various Lamb waves, rather than LCR waves that are generated using this configuration.

Investigations of the use of Lamb modes and the fundamental theory involved, which seek to provide methods for improved stress measurement have remained of interest for many years. For example, Husson[12] extended his perturbation theory for bulk waves to the analysis of surface and Lamb waves. He predicted that Lamb waves are only sensitive to symmetric stress fields. Qu and Liu[13] discussed acoustoelastic phenomena for guided waves and used the Stroh's method. They compared dispersion curves for a prestressed single plate and bonded layers and concluded that tri-layer medium are very sensitive to residual stress while single layers are less so. However, they did not offer any experimental results to validate their analysis. Chen and Wilcox[14] analyzed the relationship between load and guided wave velocity in plate and in rail-like structures using a finite element method. They also compared their results with those from an Euler-Bernoulli beam model. Lematre *et al.*[15] analyzed residual stresses in piezoelectric layers (both single

a)Electronic mail: bondlj@iastate.edu

and polylaminate) and used the Christoffel equations. They considered the circumstance when the direction of the velocity is consistent with the direction of the load. Shi *et al.*[16] developed a method to estimate biaxial loads by measuring the change in phase velocity. This method can be used for *in situ* stress detection.

Gandhi *et al.*[17] continued to investigate the theory and extended it from bulk wave acoustoelasticity to Lamb wave acoustoelasticity. They provided both numerical model data and experimental results to show how the velocities change with the variation in the loading direction. Pau and Di Scalea[18] established an analytical model for the analysis of the nonlinear response for guided waves in prestressed plates. An appropriate third-order expression which describes the strain energy of the hyperelastic body is added to the model and is seen to provide accurate results.

In all the studies discussed there remains, however, the general challenge that under many circumstances velocity changes induced by stress are relatively small and this results in the need to implement precise timing and instrumentation. In looking for increased sensitivity, this study moved to consider higher order Lamb modes and their relationship to the effects of applied stress on these waves. Model data and results of experimental measurements are given that are in good agreement, and the data demonstrate significantly higher sensitivity to stress. The results of the numerical models, where preliminary data had been previously presented,[19] showed that some higher order modes exhibit greater sensitivity to stress than for the case of the fundamental Lamb wave modes. A calibrated experimental load frame used in an earlier study to investigate stress and texture was employed in this study to load aluminum plates[20] and give data to compare with that from the models.

II. LAMB WAVE DISPERSION CURVE UNDER AXIAL LOADING

The theory for Lamb wave acoustoelasticity has been comprehensively discussed by Gandhi and his colleagues.[17] The analytical description for Lamb wave acoustoelastic can be obtained by considering both bulk wave acoustoelasticity and the anisotropic theory for Lamb waves in a thin plate. In this study the analytical approach provided by Gandhi was adopted, but with the focus being on the case when the wave velocity and the stress are perpendicular to each other. A coordinate transformation was not used in this study.

The system geometry is shown in Fig. 1, where the thickness of the plate is h, the Lamb wave spreads in the X_1 direction, and the stress is applied in the X_2 direction.

For bulk wave propagation in anisotropic medium, the equation of motion can be expressed as[21]

$$\frac{\partial}{\partial a_\beta}\left(\Gamma_{\alpha\beta\gamma\delta}\frac{\partial u_\gamma}{\partial a_\delta}\right) = \rho^0 \frac{\partial^2 u_\alpha}{\partial t^2},\tag{1}$$
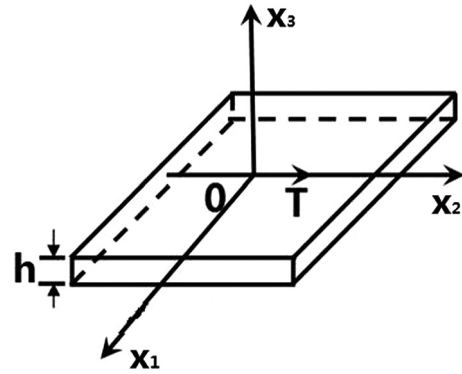
where

FIG. 1. Schematic showing coordinates for aluminum plate under uniaxial stress.

$$\Gamma_{\alpha\beta\gamma\delta} = C_{\alpha\beta\gamma\delta} + C_{\alpha\beta\lambda\delta}\frac{\partial u_\gamma^i}{\partial a_\lambda} + C_{\lambda\beta\gamma\delta}\frac{\partial u_\alpha^i}{\partial a_\lambda} + C_{\alpha\beta\gamma\delta\epsilon\zeta}e_{\epsilon\zeta}^i$$
$$ + C_{\beta\delta\epsilon\eta}e_{\epsilon\eta}^i\delta_{\alpha\gamma}.$$

e refers to the strain tensor and u represents the displacements.

The initial stress tensor in the plate can be expressed as

$$T = \begin{bmatrix} 0 & 0 & 0 \\ 0 & T_{22} & 0 \\ 0 & 0 & 0 \end{bmatrix}.\tag{2}$$

For the Lamb wave propagates in an anisotropic media, $\Gamma_{\alpha\beta\gamma\delta}$ can be simplified and given as

$$\Gamma_{\alpha\beta\gamma\delta} = C_{ijkl} + C_{jimn}e_{mn}^i\delta_{ik} + C_{ijml}e_{km}^i + C_{mjkl}e_{im}^i$$
$$ + C_{ijklmn}e_{mn}^i.\tag{3}$$

The stress and strain relationship, for bulk waves, can be written as

$$T_{\alpha\beta} = C_{\alpha\beta\gamma\delta}E_{\gamma\delta} + C_{\alpha\beta\gamma\delta\epsilon\zeta}e_{\gamma\delta}^i e_{\epsilon\eta}.\tag{4}$$

And for Lamb wave equation (4) can be simplified and written as

$$T_{\alpha\beta} = B_{\alpha\beta\gamma\delta}\frac{\partial u_k}{\partial x_l},\tag{5}$$

where

$$B_{\alpha\beta\gamma\delta} = C_{\alpha\beta\gamma\delta} + C_{\alpha\beta\epsilon\delta}e_{\delta\epsilon}^i + C_{\alpha\beta\gamma\delta\epsilon\eta}e_{\epsilon\eta}^i.$$

The form of the solution for Eq. (1) can be written as

$$u_j = U_j e^{i\omega(x_1 + \alpha x_3 - ct)},\tag{6}$$

where ω is the wavenumber for propagation in the X_1 direction, and α is the ratio of wavenumbers that are in the X_3 direction to those in the X_1 direction.

The relationship between the sixth-order tensor and Murnaghan constants l, m, and n can be written as[22]

$$C_{ijklmn} = 2\left(l - m + \frac{n}{2}\right)\delta_{ij}\delta_{kl}\delta_{mn} + 2\left(m - \frac{n}{2}\right)$$
$$\times \left(\delta_{ij}I_{klmn} + \delta_{kl}I_{mnij} + \delta_{mn}I_{ijkl}\right)$$
$$+ \frac{n}{2}\left(\delta_{ik}I_{jlmn} + \delta_{il}I_{jkmn} + \delta_{jk}I_{ilmn} + \delta_{jl}I_{ikmn}\right), \quad (7)$$

where

$$I_{ijkl} = \frac{\left(\delta_{ik}\delta_{jl} + \delta_{il}\delta_{jk}\right)}{2}.$$

The system of equations is solved using the boundary conditions for free surface stress T_{23} and T_{33} being zero at X_3 = $\pm h/2$. Following some manipulation and after a few steps, the dispersion relations for symmetric and anti-symmetric modes are given and these can be written as, for symmetric modes

$$f_s(\omega, c) = D_{11}G_1 \cot(\gamma\alpha_1) + D_{13}G_3 \cot(\gamma\alpha_3)$$
$$+ D_{15}G_5 \cot(\gamma\alpha_5) = 0. \quad (8)$$

And for anti-symmetric modes

$$f_a(\omega, c) = D_{11}G_1 \tan(\gamma\alpha_1) + D_{13}G_3 \tan(\gamma\alpha_3)$$
$$+ D_{15}G_5 \tan(\gamma\alpha_5) = 0. \quad (9)$$

Further detailed discussion and definition of the various terms used in these relationships is provided by Gandhi[17] and the parameters used in Eqs. (8) and (9) are also defined in the Appendix of this paper.

The relationships given as Eqs. (7)–(9) were used to investigate the effects of stress on different Lamb modes. The calculations utilize the relationship between the sixth-order tensor and Murnaghan constants and a MATLAB code was written to solve the equations.

III. NUMERICAL RESULTS

A. Dispersion curves under stress loading

The Lamb wave dispersion curves for plates under an axial stress can be obtained using the MATLAB code based on Eqs. (7)–(9). The code was validated with calculations using material property parameters previously reported in the literature,[17] and as a reference case a 1.0 mm thick plate is considered. Results considered the case of an aluminum plate with no-load and when the applied stress is 100 MPa. The material parameters used are shown in Table I.

The symmetric modes dispersion curves for the two cases of uniaxial stress and no-load are shown in Fig. 2. By eye it is seen that there are small differences between the results for the two cases.

B. Changes of phase velocity under stress

Validation of the code is provided through a comparison with data that has been reported in the literature,[17] and where the present calculations used as many of the same parameters as possible. Here the case considered is for the differences seen for the S_0 mode with and without stress. These

TABLE I. Aluminum parameters for calculation (Ref. 17).

Aluminum parameters for calculation		
Parameter	Value	Units
λ	54.308	GPa
μ	27.174	GPa
l	-281.5	GPa
m	-339.0	GPa
n	-416.0	GPa
ρ_0	2704	kg/m^2
v_l	6303	m/s
v_t	3102	m/s
Thickness	1	mm

difference curves are shown in Fig. 3. It is seen that the new data are in good general agreement with that from the literature. In reviewing the two cases it was found that not all parameters needed in the code (i.e., longitudinal velocity and shear velocity of 6061-T6 Aluminum) and used in the calculation were reported previously. As a result, in the present work best estimates were used for the missing data. The small differences seen between the literature and the current data are believed to be due to the values used for missing parameter data and those which were actually employed in the earlier paper.

The analysis was then extended to consider the effects of stress on higher order Lamb modes. The differences in velocity, between cases of stress and no stress, as a function of frequency for different symmetrical modes are shown in Fig. 4. As higher order modes are considered the cut-off frequencies increase (on the MHz-mm scale), and the difference seen in the phase velocity decreases. It is also seen that the S_0 mode is a special case, when compared to other modes, in that it has a peak rather than an obvious cut-off frequency.

Data for the corresponding cases of the difference in velocity for the cases of stress and no stress for different anti-symmetrical modes as a function of frequency are given as Fig. 5.

It is seen in Fig. 5 that as mode order increases from the A_1 to A_7 mode, the cut-off frequency moves to higher values on the MHz mm scale. The form of the differences for the A_0 mode is different from that for the other modes in that it has an increasing value starting from zero. The form of this
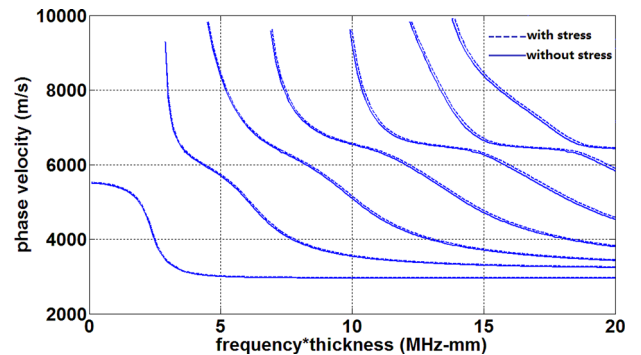

FIG. 2. (Color online) Dispersion curve for 1 mm thick aluminum plate without stress and a 100 MPa uniaxial stress.
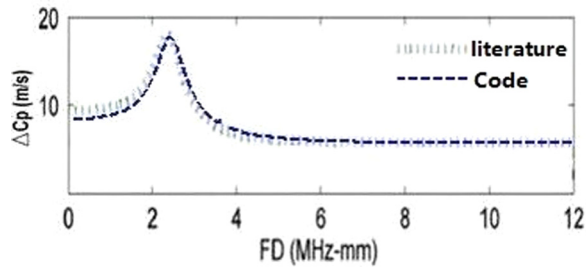
Ning Pei and Leonard J. Bond

FIG. 3. (Color online) The difference in velocity for the S_0 mode with and without stress, comparing (i) that given in the literature (Ref. 17) and (ii) results using the new code.

response is the same as results previously given in the literature.[17]

C. Changes in group velocity under stress

In an experiment it is the group velocity that is measured, and to provide data for comparison with experiments it is necessary to calculate this velocity. These data were calculated and the change seen in the group velocity under a 100 MPa uniaxial stress for the cases of the S_0, S_1, A_0, and A_1 modes are shown in Fig. 6. From the data it is seen that the S_1 mode exhibits the largest change under load at lower frequency-thickness values and that this mode appears to have the highest sensitivity to stress.

To compare sensitivity to stress for different bulk wave types and Lamb wave modes the use of velocity normalized in a frequency and thickness form at 3.0 MHz mm was selected. The relative change in velocity with load for the range of strain from 0 to 600 $\mu\varepsilon$ was calculated. The data for the cases of the S_0, S_1, A_0, and A_1 modes are shown in Fig. 7. It can be seen that the relative change of the velocity for the S_1 mode is much larger, when compared to that for other modes under the same strain.

When considering the data shown in Fig. 7, the absolute value of the slope gives a measure for velocity change sensitivity for different modes and the stress sensitivity coefficient
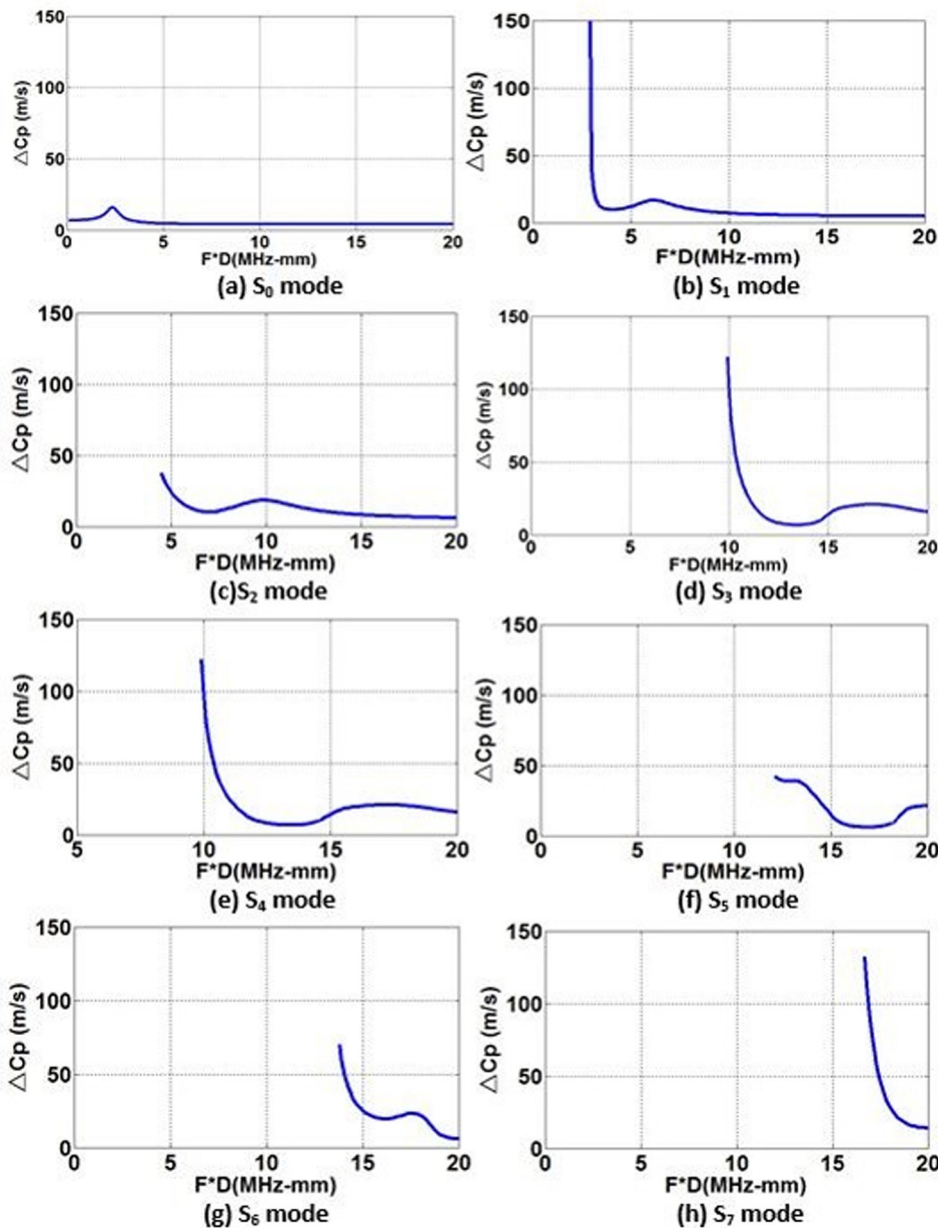

FIG. 4. (Color online) Symmetrical mode velocity difference in a 1 mm aluminum plate, as a function of frequency, between cases of 100 MPa's load and no-load.
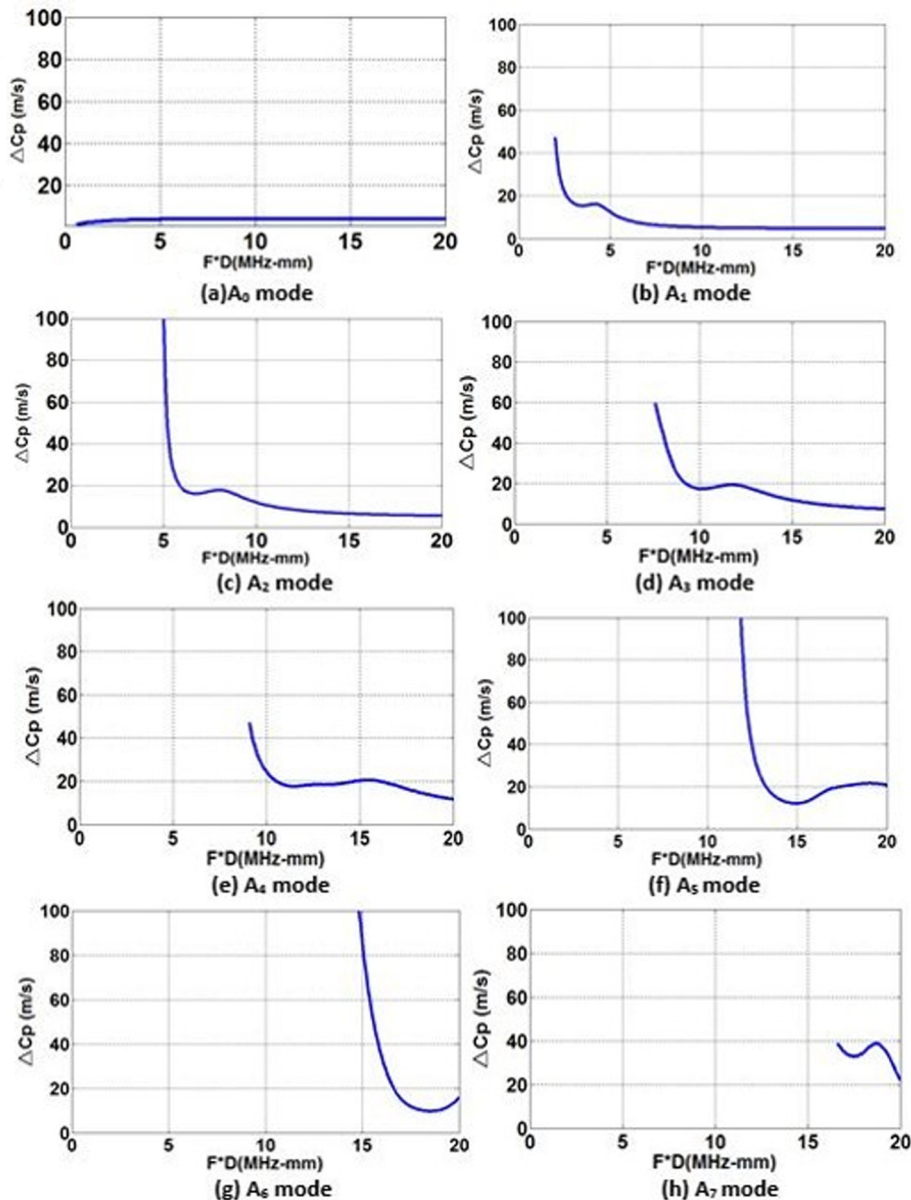
FIG. 5. (Color online) Anti-symmetrical mode velocity difference in a 1 mm aluminum plate, as a function of frequency, between cases of 100 MPa's load and no-load.

is in units of $\mu\varepsilon^{-1}$. For comparison the corresponding data for the change of velocity with strain for compressional waves in aluminum and in steel are shown in Fig. 8.

The data in Fig. 8 show that the S_1 mode Lamb wave in aluminum is about ten times more sensitive to load than for the case of a compressional wave. The sensitivity is also a function of the frequency-thickness parameter and Fig. 9 shows the sensitive coefficient for the S_1 mode. It is seen that the coefficient value is highest (most sensitive) close to 3.0 MHz mm, the cut-off frequency and it then decreases sharply as the frequency-thickness parameter increased. It does exhibit a second, but smaller peak, at a value close to that which is twice the cut-off frequency.

D. Uncertainties in the numerical calculations for velocity

Potential sources of errors and uncertainties in the numerical calculations were investigated. The most significant cause of inaccuracy and errors would appear to be due

to the values for the input parameters used. The sensitivity of variation in material parameters was investigated by repeating calculations when changing values of one parameter by 5% and 1%, and the effect of these changes on relative change in velocity are tabulated in Table II.

As is seen with the data in Table II, when changing the values of the input parameters used for λ and μ change in turn by 1%, give changes in the "relative change of velocity" by 12.75% and 21.9%, respectively. If reliable calculations of estimates for stress are to be obtained from changes in velocity, it is essential to use the best available material property data set for the base material.

IV. EXPERIMENT RESULTS

A. Experiment setup

In order to provide velocity data to compare with the model estimates for higher order plate wave modes sensitivity to stress it is necessary to have sheet samples with
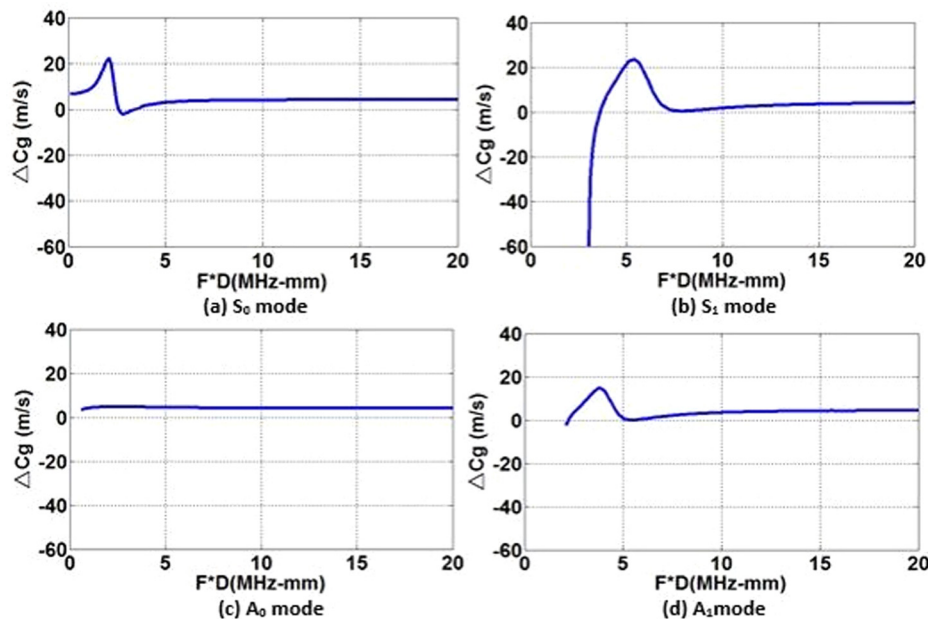
Ning Pei and Leonard J. Bond

FIG. 6. (Color online) The differences in group velocity for the S_0, S_1, A_0, and A_1 modes as a function of frequency, between no-load and with 100 MPa stress applied.

controlled loads. To achieve this, a previously constructed load frame was dedicated to this project.[20] This system is shown in Fig. 10. It incorporates a manual two speed hydraulic hand pump that can deliver loads up to 27 000 kg. This load is applied to samples with a 6.45 cm^2 section, which gives loads of up to about 400 MPa. Samples were aluminum sheets 1.6 mm thick, with length and width of approximately 50 and 45 cm, respectively. Load is applied to the sheet samples with clamps that attach to bolts set into precision drilled double rows of 17 holes. The resulting loads were measured using three strain gages with a P3 Strain Indicator and Recorder (Vishay Measurements Group, Inc., Wendell, NC). The strain gages were attached to the aluminum plate with their axis set to be in the same direction as the uniaxial loading. The strain was recorded using the P3 Strain Indicator and Recorder.
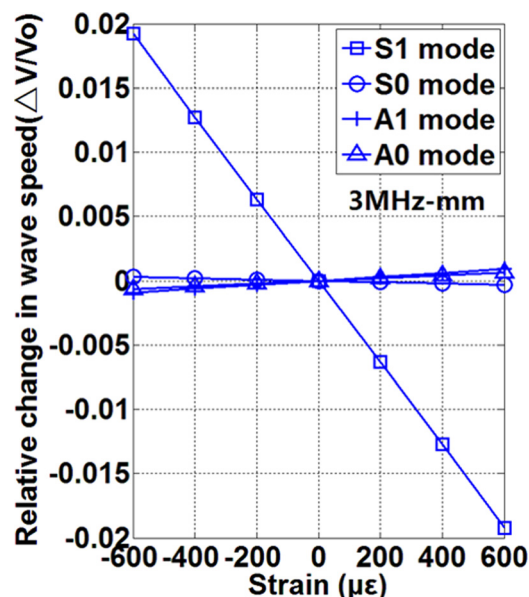
The ultrasonic plate wave measurement system is comprised of oblique wedges set in a yoke to ensure that they maintain constant separation. The transducers were 2.25 MHz compression wave (Panametrics, type A404, South Burlington, VT). Lamb waves are generated and received by using the transducers fastened onto variable-angle Plexiglas wedges, as shown in Fig. 11.

The transmitter is driven using a tone burst signal generator (Hewlett Packard 33120A, Renton, WA) and a high power amplifier (Model 3100L, Electronic Navigation Industry, Rochester, NY). The receiver is connected to a pre-amplifier (Olympus, Waltham, MA), giving 50 dB of gain, and signals

FIG. 7. (Color online) The change of group velocity for S_0, S_1, A_0, and A_1 modes with strain under and at a normalized thickness—frequency combination, 3 MHz mm, in an aluminum plate.
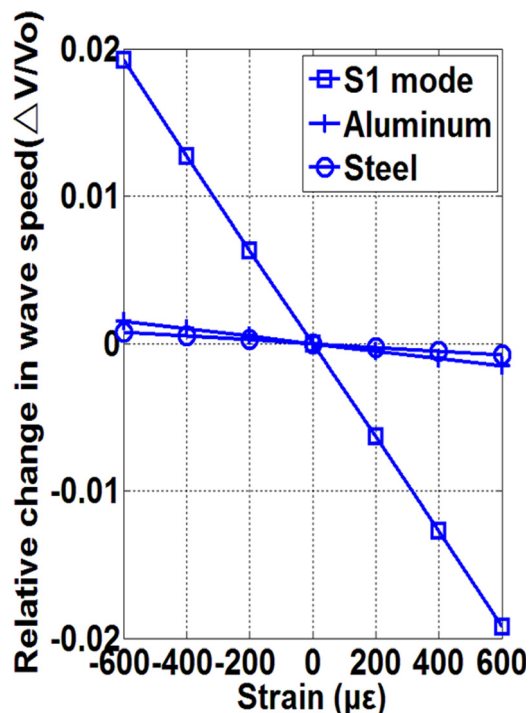

FIG. 8. (Color online) The change of velocity with strain of compressional wave for aluminum (Ref. 7) and for steel (Ref. 23) compared with data for the S_1 mode in aluminum.

J. Acoust. Soc. Am. **140** (5), November 2016

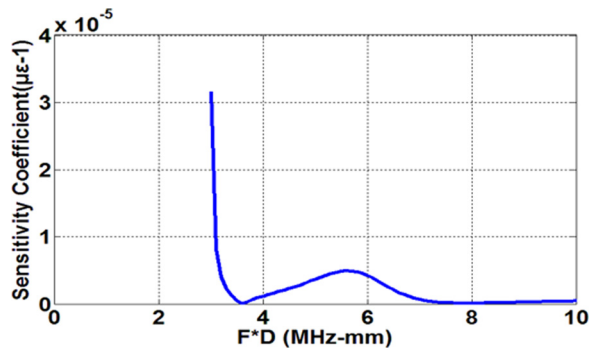Ning Pei and Leonard J. Bond   3839

FIG. 9. (Color online) Sensitive coefficient for the S_1 mode, as function of normalized frequency-thickness product.

measured with a digital oscilloscope (HDO4022, 200 MHz High Definition Oscilloscope, Teledyne LeCroy, Chestnut Ridge, NY). The system is used to apply a 30 cycle tone burst, with a selected frequency, which is typically at or close to the cut-off frequency. The transmitter is used to generate a specific mode in the plate. The incident angle needed for each mode is identified using Snell's law and the Lamb wave's phase velocity dispersion curve. For the case of the S_1 mode, as shown in Fig. 12, variation in frequency results in a change in velocity. Mineral oil is used as the couplant between the oblique wedge and aluminum plate. A constant pressure is applied to the transducer-receiver system to ensure that consistent coupling is maintained. The received signal is amplified and input into the oscilloscope, digitized at a 100 MHz sampling rate, averaged 64 times to improve the signal-to-noise ratio, and saved for subsequent signal processing.

An example of a typical received signal is shown as Fig. 13. In this case there are four modes in the received signal. These can be identified, by their velocities, as corresponding to the A_1 mode, which is the fastest, and the S_1 mode, which is the slowest. The various modes that are observed are in agreement with those predicted for the dispersion curve near 3.0 MHz mm.

B. Experiment data analysis

The use of a short-time Fourier transform (STFT) has been demonstrated to be an effective method for use in dispersive curve analysis.[24–26] It has been reported that the arrival time for group velocity at specific frequencies can be obtained by determining the magnitude of the coefficients. The theory and physical meaning of STFT derived data are discussed in the literature.[25,26]

TABLE II. Influence of parameters to the calculated results.

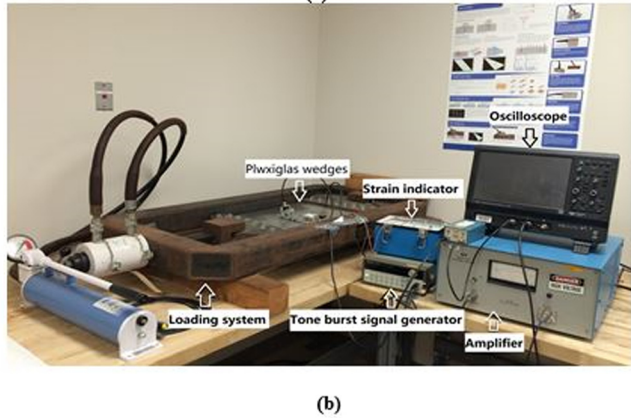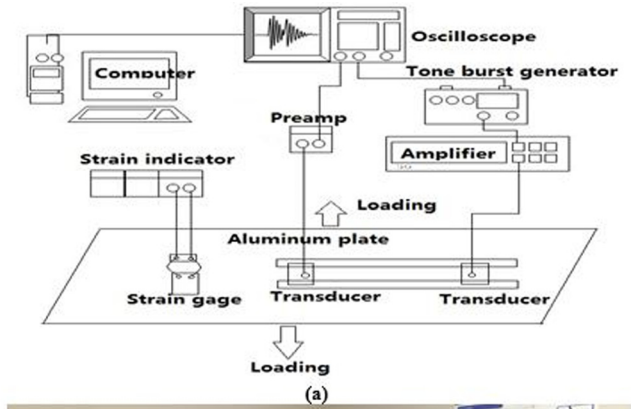|	Influence of aluminum parameters for calculation	
Parameter	Value change 5%	Value change 1%
λ	42.44%	12.75%
μ	54.26%	21.9%
l	2.34%	0.48%
m	1.84%	0.325%
n	7.05%	1.35%

(a)

(b)

FIG. 10. (Color online) Tone burst generator used for the experiment system (a) system schematic (b) photograph of the complete system.

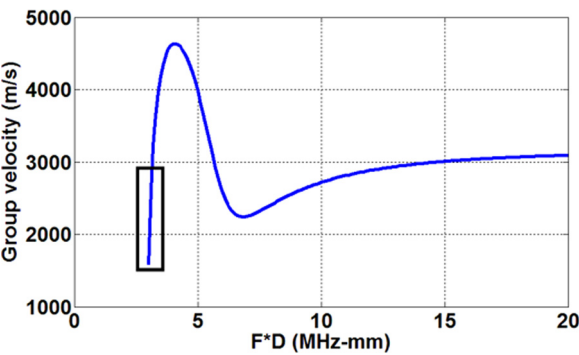FIG. 11. (Color online) Transmission mode used in the experiment.

FIG. 12. (Color online) S_1 mode group velocity dispersion curve.
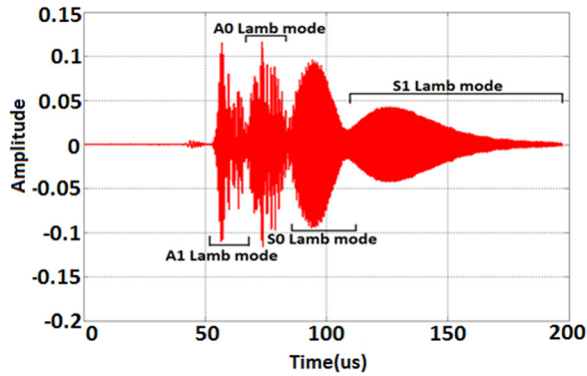
Ning Pei and Leonard J. Bond

FIG. 13. (Color online) An example of a received signal for 3 MHz-mm on an aluminum plate.

In using this approach the steps involved in identifying arrive times by STFT are

(1) Apply the STFT algorithm.
(2) Identifying the time slice corresponding to the amplitude at the center frequency.
(3) Record the time constant, which gives the arrival time t_1 of the Lamb with the largest amplitude in the time slice. Changing transducer separation d, recording the arrival time t_2. The group velocity of the Lamb wave at the center frequency can then be obtained by dividing the distance d by the time difference $t = t_2 - t_1$.
(4) The Lamb wave group velocity at different frequency can then be obtained by adjusting the center frequency for the incident signal.

The group velocity for different modes can be obtained by variation of the wedge angle, where the angle is selected, based on Snell's law. When a range of different group velocity data are obtained for various modes at different frequencies, the Lamb wave group velocity dispersion curve is obtained.

The STFT algorithm is used for the time-frequency analysis. An example of the data obtained corresponding to the S_1 Lamb mode is shown as Fig. 14. It gives a representation for the time domain and frequency information at the same time. The energy is seen to be concentrated near 1.9 MHz.

Following characterization of the S_1 Lamb wave the effects of applying a load to the aluminum plate were
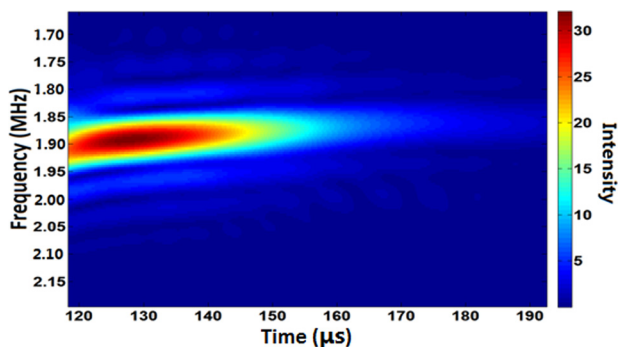

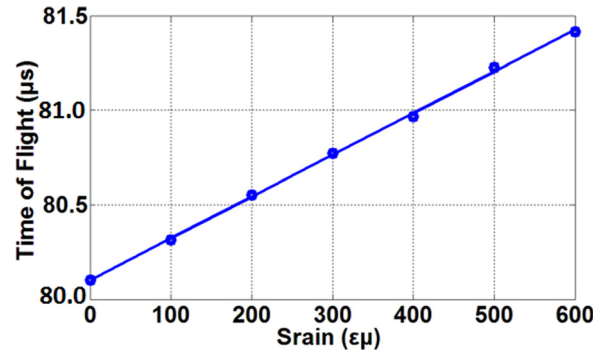FIG. 14. (Color online) Time-frequency analysis of S_1 mode for the sample aluminum plate.

FIG. 15. (Color online) Time of flight at various strains for the S_1 mode.

investigated. Recording the arrival time t_1 and then, changing transducer separation d, applying pressure with distance d and then record the transit time t_2'. The group velocity of the Lamb wave at the center frequency can then be obtained by dividing the distance d by the time difference $t' = t_2' - t_1$. The load was monitored using the strain gages and velocity/arrival time values monitored as the load was increased. The time domain data were recorded from 0 to 600 $\mu\varepsilon$, with the interval of 100 $\mu\varepsilon$. The measurements were each performed six times and the average strain and time-of-flight (TOF) data were recorded. Figure 15 gives an example of data showing the time of flight for the S_1 mode, with the change of strain, the data show a linear relationship. For each data point the relative change in velocity for the S_1 mode, over the velocity at zero loading, was calculated. The model and experimental data (red) at 3.0 MHz mm are plotted against strain and is shown as Fig. 16. It is seen that the absolute value of slope of the experiment data is 2.72×10^{-5} $\mu\varepsilon^{-1}$, which is a little less than that for the model result data (3.25 $\mu\varepsilon^{-1}$). For the data the measurements are performed six times and their mean ($\bar{x}$) is regarded as a good estimation of the true value, the error bars can be expressed as standard deviation (σ) and standard error ($S = \sigma/\sqrt{N}$). These values
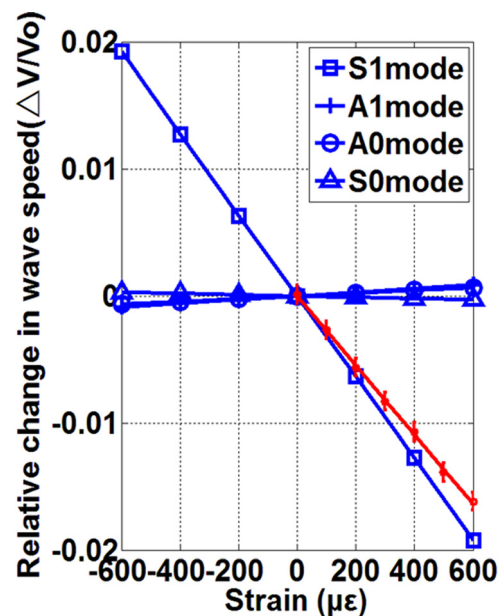

FIG. 16. (Color online) Comparison of experiment and model data for velocity change against strain with the experiment data (red).
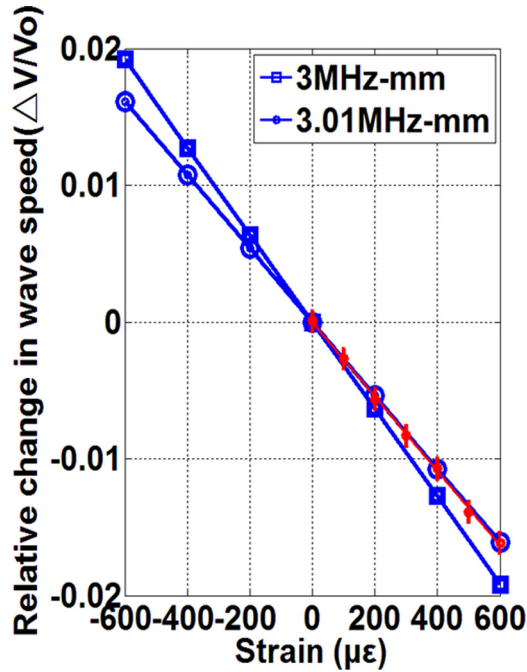
FIG. 17. (Color online) Comparison of experiment S_1 velocity change against load and numerical model results for cases at 3.0 and 3.01 MHz mm.

are used as the standard error for the error bars, with the results shown in Fig. 16 where $\bar{x} \pm S$.

When the S_1 mode velocity was investigated it was found to be less sensitive than that predicted for the cut-off at the 3.0 MHz mm. Upon review of the data in Fig. 13, the S_1 dispersion curve, the velocity showed that the wave actually generated experimentally was most probably not at the cutoff. It would appear that the experimental data more accurately corresponded to the case of S_1 at 3.01 MHz mm. The model data for the S_1 mode at 3.00 and 3.01 MHz mm at various loads, together with the experimental data are shown in Fig. 17. The data are seen to be in good agreement. Here the error bars are obtained the same method as used for Fig. 16 where the data were measured six times and averaged, with standard errors used to give the error bar.

V. CONCLUSIONS

For Lamb wave propagation in the direction perpendicular to the direction of applied stress, the sensitivity of both symmetrical and anti-symmetrical modes to stress was studied. In terms of effect on velocity it is the change

in velocity for the S_1 mode that exhibits significantly higher sensitivity to stress than other Lamb modes. For aluminum, the use of the S_1 mode for stress measurement is found to be about ten times more sensitive than the traditional bulk wave measurements, and the fundamental Lamb were modes. The use of higher order Lamb modes offers a new approach to stress measurement in plate and there is potential for techniques for new and improved online industrial stress measurement.

ACKNOWLEDGMENTS

APPENDIX

The values of the various constants used in the model follow those given by Ghandi et al.[17]

These relationships are obtained by substitution of Eq. (6) into Eq. (1), to give the expression shown in the form

$$K_{mn}(\alpha)U_n = 0, \tag{A1}$$

where K_{mn} are expressed as

$$
\begin{aligned}
K_{11} &= c^2\rho^0 - A_{1111} - \alpha^2 A_{1313}, \\
K_{22} &= c^2\rho^0 - A_{1212} - \alpha^2 A_{2323}, \\
K_{33} &= c^2\rho^0 - A_{1313} - \alpha^2 A_{3333}, \\
K_{12} &= K_{21} = -A_{1112} - \alpha^2 A_{1323}, \\
K_{13} &= K_{31} = -\alpha(A_{1133} + A_{1331}), \\
K_{23} &= K_{32} = -\alpha(A_{1233} + A_{1332}).
\end{aligned}
$$

In order to obtain non-trivial solutions for the displacement U_n, the determinant of the matrix K_{mn} must go to zero, which can lead to a sixth-order equation about α_q, $q = 1, \ldots, 6$. The expression is as shown in Eq. (A2) with the odd powers of α all zero

$$P_6\alpha^6 + P_4\alpha^4 + P_2\alpha^2 + P_0 = 0, \tag{A2}$$

where

$$
\begin{aligned}
P_6 &= (A_{1323}^2 - A_{1313}A_{2323})A_{3333}, \\
P_4 &= A_{1233}^2 A_{1313} + A_{1313}A_{1323}^2 - 2A_{1133}A_{1323}A_{1332} - 2A_{1323}A_{1331}A_{1332} + A_{1313}A_{1332}^2 \\
&\quad + 2A_{1233}(-A_{1323}(A_{1133} + A_{1331}) + A_{1313}A_{1332}) + A_{1133}^2 A_{2323} - A_{1313}^2 A_{2323} + 2A_{1133}A_{1331}A_{2323} \\
&\quad + A_{1331}^2 A_{2323} - (A_{1212}A_{1313} - 2A_{1112}A_{1323} + A_{1111}A_{2323})A_{3333} + c^2\rho_0(-A_{1323}^2 + A_{1313}A_{2323}) \\
&\quad + (A_{1313} + A_{2323})A_{3333},
\end{aligned}
$$

Ning Pei and Leonard J. Bond

$$P_2 = A_{1133}^2 A_{1212} + A_{1111} A_{1233}^2 - A_{1212} A_{1313}^2 + 2A_{1112} A_{1313} A_{1323} - 2A_{1112} A_{1233} A_{1331} + A_{1212} A_{1331}^2$$
$$+ 2A_{1111} A_{1233} A_{1332} - 2A_{1112} A_{1331} A_{1332} + A_{1111} A_{1332}^2 - 2A_{1133}(-A_{1212}A_{1331} + A_{1112}(A_{1233} + A_{1332}))$$
$$- A_{1111}A_{1313}A_{2323} + (A_{1112}^2 - A_{1111}A_{1212})A_{3333} - c^4\rho_0^2(A_{1313} + A_{2323} + A_{3333}) + c^2\rho(-2A_{1112}A_{1323} - (A_{1133} + A_{1331})^2$$
$$- (A_{1233} + A_{1332})^2 + A_{1313}(A_{1212} + A_{1313} + A_{2323}) + A_{1212}A_{3333} + A_{1111}(A_{2323} + A_{3333})),$$
$$P_0 = (-A_{1112}^2 + (c^2\rho_0 - A_{1111})(c^2\rho_0 - A_{1212}))(c^2\rho_0 - A_{1313}).$$

Displacement ratios of U_2 and U_3 to U_1 for each of the six values of α:

$$V_q = \frac{U_{2q}}{U_{1q}}, \quad W_q = \frac{U_{3q}}{U_{1q}}, \quad q = 1, 2, \ldots, 6. \qquad \text{(A3)}$$

The total displacement field of the Lamb wave in three different directions can be written as

$$\{u_1, u_2, u_3\} = \sum_{q=1}^{6} \{1, V_q, W_q\} U_{1q} e^{i\xi(x_1 + \alpha_q x_3 - ct)}. \qquad \text{(A4)}$$

Insert Eq. (A4) into Eq. (5), the stress components in the x_3 direction can be written as

$$\{T_{33}, T_{13}, T_{23}\} = \sum_{q=1}^{6} i\xi\{D_{1q}, D_{2q}, D_{3q}\} U_{1q} e^{i\xi(x_1 + \alpha_q x_3 - ct)},$$
$$\text{(A5)}$$

where the parameters D_{mq} are given by

$$D_{1q} = B_{3311} + B_{3312}V_q + \alpha_q B_{3333}W_q,$$
$$D_{2q} = \alpha_q(B_{1313} + B_{1323}V_q) + B_{1331}W_q,$$
$$D_{3q} = \alpha_q(B_{1323} + B_{2323}V_q) + B_{1332}W_q.$$

Considering the boundary conditions, follow some manipulation and with a few steps, the dispersion relationships (8) and (9) can be obtained. Further detailed discussion is provided by Gandhi.[17]

[1]D. Ensminger and L. J. Bond, *Ultrasonics: Fundamentals, Technologies and Application*, 3rd ed. (CRC Press, Boca Raton, FL, 2011), Chap. 8, pp. 305–365.

[2]F. D. Murnaghan, *Finite Deformation of an Elastic Solid* (Wiley, New York, 1951), pp. 1–118.

[3]D. S. Hughes and J. L. Kelly, "Second-order elastic deformations of solids," Phys. Rev. **92**, 1145–1149 (1953).

[4]Y.-H. Pao, W. Sachse, and H. Fukuoka, "Acoustoelasticity and ultrasonic measurement of residual stress," in *Physical Acoustics*, edited by W. P. Mason and R. N. Thurston (Academic, New York, 1984), Vol. XVII, pp. 61–143.

[5]D. I. Crecraft, "The measurement of applied and residual stresses in metals using ultrasonic waves," J. Sound. Vib. **5**(1), 173–192 (1967).

[6]F. A. Kandil, J. D. Lord, A. T. Fry, and P. V. Grant, "A review of residual stress measurement methods—A guide to technique selection," National Physical Laboratory (NPL) Report MATC (A)**04**, pp. 1–42 (2001).

[7]N. S. Rossini, M. Dassisti, K. Y. Benyounis, and A. G. Olabi, "Methods of measuring residual stresses in components," Mater. Des. **35**, 572–588 (2012).

[8]A. V. Clark, Jr. and J. C. Moulder, "Residual stress determination in aluminium using electromagnetic acoustic transducers," Ultrasonics **23**(6), 253–259 (1985).

[9]D. E. Bray and P. Junghans, "Application of the LCR ultrasonic technique for evaluation of post-weld heat treatment in steel plate," NDT&E Int. **28**(4), 235–242 (1995).

[10]F. Belahcene and J. Lu, "Determination of residual stress using critically refracted longitudinal waves and immersion mode," J. Strain Anal. **37**(1), 13–20 (2002).

[11]D. E. Bray and W. Tang, "Subsurface stress evaluation in steel plates and bars using the LCR ultrasonic wave," Nucl. Eng. Des. **207**(2), 231–240 (2001).

[12]D. Husson, "A perturbation theory for the acoustoelastic effect of surface waves," J. Appl. Phys. **57**(5), 1562–1568 (1985).

[13]J. Qu and G. Liu, "Effects of residual stress on guided waves in layered media," in *Review of Progress in Qualitative Nondestructive Evaluation*, edited by D. O. Thompson and D. E. Chimenti (Plenum, New York, 1998), Vol. 17B, pp. 1635–1642.

[14]F. Chen and P. D. Wilcox, "The effect of load on guided wave propagation," Ultrasonic **47**(1-4), 111–122 (2007).

[15]M. Lematre, G. Feuillard, T. Delaunay, and M. Lethiecq, "Modeling of ultrasonic wave propagation in integrated piezoelectric structures under residual stress," IEEE Trans. Ultrason. Ferroelectr. Freq. Control **53**(4), 685–696 (2006).

[16]F. Shi, J. E. Michaels, and S. J. Lee, "*In situ* estimation of applied biaxial loads with Lamb waves," J. Acoust. Soc. Am. **133**(2), 677–687 (2013).

[17]N. Gandhi, J. E. Michaels, and S. J. Lee, "Acoustoelastic Lamb wave propagation in biaxially stressed plates," J. Acoust. Soc. Am. **132**(3), 1284–1293 (2012).

[18]A. Pau and F. L. di Scalea, "Nonlinear guided wave propagation in prestressed plates," J. Acoust. Soc. Am. **137**(3), 1529–1540 (2015).

[19]N. Pei and L. J. Bond, "Acoustoelastic Lamb wave analysis in thin plate," in *Proceedings IEEE Far East NDT New Technology and Application Forum (FENDT)*, Zhuhai, China (May 28–31, 2015), pp. 149–153.

[20]S. J. Wormley and R. B. Thompson, "Development of a breadboard instrument for the ultrasonic measurement of stress," in *Review of Progress in Qualitative Nondestructive Evaluation*, edited by D. O. Thompson and D. E. Chimenti (Plenum, New York, 1989), Vol. 8, pp. 1119–1125.

[21]Y.-H. Pao and U. Gamer, "Acoustoelastic wave in orthotropic media," J. Acoust. Soc. Am. **77**, 806–812 (1985).

[22]N. Gandhi, "Determination of dispersion curves for acoustoelastic Lamb wave propagation," Master's thesis, Georgia Institute of Technology, Atlanta, GA, 2010, pp. 1–73.

[23]D. M. Egle and D. E. Bray, "Measurement of acoustoelastic and third-order elastic constants for rail steel," J. Acoust. Soc. Am. **60**(3), 741–744 (1976).

[24]M. Niethammer, L. J. Jacobs, J. Qu, and J. Jarzynski, "Time-frequency representations of Lamb waves," J. Acoust. Soc. Am. **109**(5), 1841–1847 (2001).

[25]K. Kishimoto, H. Inoue, M. Hamada, and T. Shibuya, "Time frequency analysis of dispersive waves by means of wavelet transform," J. Appl. Mech. Vol. **62**(4), 841–846 (1995).

[26]L. Wang and F. G. Yuan, "Group velocity and characteristic wave curves of Lamb waves in composites: Modeling and experiments," Compos. Sci. Technol. **67**(7-8), 1370–1384 (2007).